

## A comparative study of the stress-dependence of dynamic and static moduli for sandstones with different porosities

Yang Wang\*, De-hua Han, and Jiali Ren, Rock Physics Lab, University of Houston; Hui Li, School of Electronic and Information Engineering, Xi'an Jiaotong University; Yonghao Zhang, CNPC Logging Co., Ltd

### Summary

We present the dynamic and static moduli measured in hydrostatic and triaxial load-unload processes for three sandstones with different porosities. In contrast to dynamic moduli, the statically derived ones show more sensitivity to the elevated pressure or stress. With a comparative analysis together with the modified Voigt-Reuss bounds, porosity, the rock intrinsically have, determines the variability of the static moduli, which decreases with the increasing porosity. Moreover, the static moduli are highly dependent on the stress path or history. In general, the unloading bulk modulus is almost always larger than the loading one. For Young's modulus, the unloading modulus is much higher than the loading one at high stress, while the relation is reversed at low stress level.

### Introduction

Within geoscience and geoengineering, it is customary to differentiate between dynamic and static elastic moduli. Dynamic moduli, derived from the laboratory and well log measurements, reflect much broader reservoir properties, while static moduli are more representative of the in-situ reservoir deformation. It is suitable to predict the static moduli by using the dynamic moduli as inputs after proper corrections. But the conversion from dynamic to static properties is not straightforward. Some influential factors should be carefully taken into account.

For most sedimentary rocks, the mineral grains keep intimate contacts with neighboring grains to form the solid frame. The presence of grain boundaries and intergranular micro-cracks is unavoidable (Tutuncu et al., 1998). With external stress, these granular microstructures may induce some non-elastic processes, leading to the nonlinear strain responses. Numerous studies have suggested that the static elastic modulus for room-dry rocks is almost always lower than the dynamically derived one, especially at low stress levels (Simmons and Brace, 1965; King, 1969; Li et al., 2019). The reason for this discrepancy can be attributed to these non-elastic processes which create more effects on the static tests with strain amplitude ( $10^{-3}$ ) orders of magnitude larger than that induced by the ultrasonic wave propagation ( $10^{-6}$ ) (Fjaer, 2019). Because of the complexity of porous medium, the stress sensitivity of the granular structures may vary from one rock to another. Additionally, the induced non-elastic processes are strongly dependent on the stress path or history.

In this research, we select three sandstone samples with different porosities to comparatively investigate the stress sensitivity and stress history dependence of the dynamic and static moduli under both hydrostatic and triaxial stress conditions.

### Sample descriptions and experimental set-up

The porosity for three sandstone samples (Idaho Gray, Berea, Tight) is 33.31%, 23.22%, and 4.86%, respectively. Three samples are cut cylindrically with the length of around 5.0cm and the diameter of around 3.7cm. The ends of the cores are ground flat within  $\pm 2.5 \times 10^{-3}$  cm.

A servo-controlled rock mechanics test system (AutoLab 1500 from New England Research Inc.) has been used for the measurements. The cylindrical samples are wrapped with rubber sleeves and placed between two endcaps. Each endcap has been equipped with piezoelectric transducers to measure the vertical P- and S-wave velocities. The central frequency of both P- and S-wave transducers is 1.0MHz. The ultrasonic velocity is calculated from the first arrival time and the sample length after being corrected throughout the loading and unloading. Moreover, two linear variable differential transformers (LVDT) are clamped at the end of two endcaps to measure the axial displacements, while another pair of LVDTs is mounted at the mid-length of the sample to measure the radial displacements. Axial and radial strains are derived from those measured displacements.

Tests are conducted at room-dry condition and pore pressure is assumed to be negligible. All three samples are subjected to hydrostatic and deviatoric load-unload processes. The hydrostatic tests are controlled with a constant stress rate of 0.2MPa/s, while the triaxial tests are performed at a constant stress rate of 0.02 MPa/s. It should be noted that we use the term deviatoric stress to represent the difference between the axial and radial stresses.

By assuming isotropic materials, the dynamic bulk modulus ( $K_{dyn}$ ) and Young's modulus ( $E_{dyn}$ ) can be expressed as functions of the P- and S-wave velocities (i.e.,  $V_p$  and  $V_s$ ) and the density  $\rho$ :

$$K_{dyn} = \rho(V_p^2 - \frac{4V_s^2}{3}) \quad (1)$$

$$E_{dyn} = \rho V_p^2 (\frac{3V_p^2 - 4V_s^2}{V_p^2 - V_s^2}) \quad (2)$$

## Static and dynamic moduli

The static bulk modulus ( $K_{\text{stat}}$ ) and Young's modulus ( $E_{\text{stat}}$ ) are derived as the ratio between mean stress ( $\sigma_{\text{mean}}$ ) and volumetric strain ( $\epsilon_{\text{vol}}$ ) increments during hydrostatic tests or the ratio between axial stress ( $\sigma_a$ ) and axial strain ( $\epsilon_a$ ) increments during triaxial tests, respectively:

$$K_{\text{stat}} = \frac{\Delta\sigma_{\text{mean}}}{\Delta\epsilon_{\text{vol}}} \quad (3)$$

$$E_{\text{stat}} = \frac{\Delta\sigma_a}{\Delta\epsilon_a} \quad (4)$$

### Experimental results and analysis

#### 1. Nonlinear strain responses

Figure 1 shows the relationships between the volumetric strain ( $\epsilon_{\text{vol}}$ ) and the hydrostatic stress ( $\sigma_{\text{mean}}$ ) in a load-unload cycle. The volumetric strain is defined as:  $\epsilon_{\text{vol}} = \epsilon_a + 2\epsilon_r$ , where  $\epsilon_a$  is the axial strain and  $\epsilon_r$  is the radial strain. The peak stress is 20MPa for Idaho Gray sandstone and 40MPa for Berea and Tight sandstones, respectively. From the whole, regardless of being from the loading or unloading phase, the stress-strain curves are not perfectly linear, especially at relatively low pressure conditions. The unloading curves are much steeper than the loading curves. This might be attributed to that the loading strain is the sum of elastic and plastic strains while the unloading strain represents a relatively elastic response to pressure (Fjaer, 2009). Additionally, after removing the applied pressure, the unloading curves do not get back to the origins, and there are obvious hysteresis between loading and unloading. In contrast, at the same peak pressure level, Berea sandstone exhibits more hysteresis than Tight sandstone, which might be attributed to the much larger porosity of Berea sandstone.

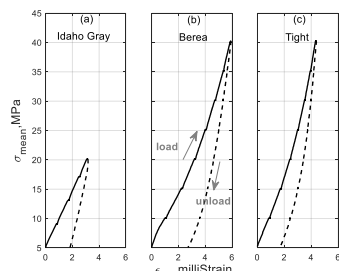


Figure 1: The volumetric strain ( $\epsilon_{\text{vol}}$ ) as a function of the mean stress ( $\sigma_{\text{mean}}$ ) in a load-unload cycle for (a) Idaho Gray sandstone, (b) Berea sandstone, and (c) Tight sandstone.

Figure 2 shows the axial strain ( $\epsilon_a$ ) as a function of the deviatoric stress ( $\sigma_d$ ). Considering that Idaho Gray sandstone is relatively soft, only one low-stress cycle is set up with the peak stress of ~20MPa. Two deviatoric cycles are performed for the rest two samples: one low-stress cycle with the peak stress of ~30MPa, one high-stress cycle with the peak stress of ~50MPa for Berea sandstone and ~60MPa for Tight sandstone.

For all three samples, the axial strains respond nonlinearly to the deviatoric stress. The unloading curves do not follow the loading curves whatever during the 1<sup>st</sup> load-unload or the 2<sup>nd</sup> load-unload, leading to obvious hysteresis. This might be explained by the energy loss used for grain compaction and frictional slips. In addition, at the same stress level, the relation for the axial strain of three samples is: Idaho Gray > Berea > Tight, which means that porosity might be the first-order factor dominating how much the rock is deformed.

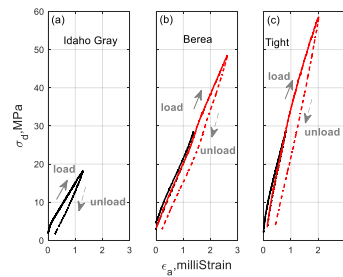


Figure 2: The axial strain ( $\epsilon_a$ ) as a function of the deviatoric stress ( $\sigma_d$ ) in load-unload loops for (a) Idaho Gray sandstone, (b) Berea sandstone, and (c) Tight sandstone.

#### 2. Dynamic and static bulk moduli

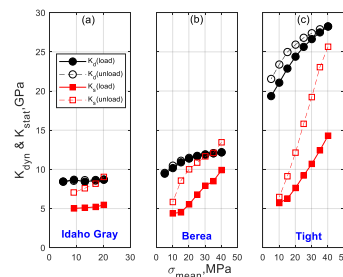


Figure 3. Dynamic and static bulk moduli (i.e.,  $K_{\text{dyn}}$  and  $K_{\text{stat}}$ ) as a function of the mean stress ( $\sigma_{\text{mean}}$ ) in the hydrostatic load-unload for three samples.

Figure 3 shows the evolutions of dynamic and static bulk moduli with pressure load and unload. Both dynamic and static moduli increase with pressure load. In contrast to the dynamic modulus, the static one exhibits more variations from the very beginning to the peak pressure. When the pressure initially reversed, the static bulk modulus jumps to a much higher value which is approaching the dynamic counterpart. The unloading moduli are much higher than the loading ones statically and dynamically. It should be noted that Idaho Gray sandstone with the highest porosity displays very small modulus changes with pressure. From the whole, the dynamic bulk modulus can be treated as the upper bound of the static one at almost any pressure state.

#### 3. Dynamic and static Young's moduli

## Static and dynamic moduli

Figure 4 exhibits the dynamic and static Young's moduli as a function of the deviatoric stress at different stress cycles. In the 1<sup>st</sup> load-unload cycle, the dynamic moduli nearly keep constant for Idaho Gray sandstone and show increasing trends with the elevated stress for Berea and Tight sandstones. In the 2<sup>nd</sup> load-unload cycle, the dynamic moduli initially increase along the trend in the 1<sup>st</sup> load. After a certain stress level, they begin to decrease with the increasing stress, and the unload moduli obviously are lower than the load moduli, indicating irrecoverable deformations in the 2<sup>nd</sup> cycle for Berea and Tight sandstones.

In the 1<sup>st</sup> load, the static Young's moduli of three samples display decreasing trends. When the load is initially reversed, the static modulus instantaneously jumps to a value approaching the dynamic modulus. As the unloading process continues, the static modulus hence decreases from a much higher value. In the 2<sup>nd</sup> load-unload cycle, the static moduli firstly follow the decreasing trends in the 1<sup>st</sup> load. When the deviatoric stress is beyond the peak stress in the first cycle, the static moduli continue to decrease with the elevated stress. In each cycle, the static moduli tend to exhibit a bowknot-shaped trajectory, as shown in Figure 4. These trends mean that the unload moduli are higher than the load moduli at high stress level, while the relation between them is reversed at low stress level.

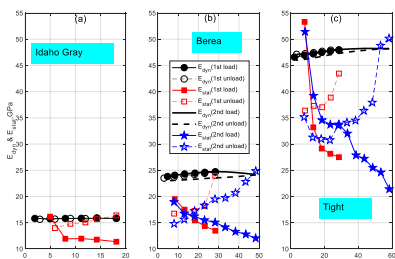


Figure 4. Dynamic and static Young's moduli (i.e.,  $E_{\text{dyn}}$  and  $E_{\text{stat}}$ ) as a function of the deviatoric stress in different load-unload cycles for three samples.

In contrast to the trends of dynamic moduli, the static moduli for all samples show wider ranges of variation with stress load and unload. At the initial load or unload, sometimes the static moduli even are higher than the dynamic counterparts. For real sandstones, the grain contacts are not perfectly smooth but with asperities. At the initial load or unload, these asperities may be interlocked together, which possibly contributes to the abnormally high moduli. Although both dynamic and static moduli are strongly dependent on the stress level and stress history, the dynamic modulus can serve as the upper bound of the static counterpart.

## Discussions

### 1. Stress-dependence of the elastic moduli

Regardless of being from the hydrostatic tests or the triaxial tests, the dynamic elastic modulus is almost always higher than the statically derived one at any stress level. Both the dynamic and static moduli increase with the elevated pressure in the hydrostatic load. However, the dynamic modulus increases, while the static one decreases with the increasing stress in the deviatoric load.

In a heterogeneous material like a sedimentary rock, the surfaces of grain contacts are not perfectly smooth, but are with asperities. In the hydrostatic load, the granular microstructures will be possibly altered by the Hertzian compaction and soft pore compaction. The enlarged grain contact area, the increasing coordinate number, and the closure of pre-existing microcracks would together result in the increasing trends of the static bulk moduli.

After the hydrostatic tests, the confining pressure is kept at 20MPa. The forces around grain contacts are in equilibrium conditions. The applied deviatoric stress attempts to break these balances. The nature of the deviatoric stress is such that contacts will tend to open if they are parallel to the stress and to close if they are normal to it. The normal stress at the contact area is proportional to the external stress. In addition, the shear stress at the contacts is proportional to the normal stress according to the Coulomb theory (Jaeger et al., 2009). Once the shear stress is large enough, static friction holding grains together will be converted to dynamic friction, which induces frictional slips along grain contacts. Because of the heterogeneity of the sedimentary rocks, at a fixed stress, the above processes will show up at those asperities for which the shear force is larger than the friction force. The rest asperities will not slip. With applying more deviatoric stress, more and more of the above events would occur and the static Young's moduli show decreasing trends.

Moreover, a stress increment has an enhanced effect on the static moduli. The strain amplitude for the static tests is  $10^{-3}$ , which is orders of magnitude greater than that induced by ultrasonic wave propagation ( $10^{-6}$ ) during the dynamic tests. As the statement from Winkler et al. (1979), the frictional sliding nearly has no effect on the measurements with strain amplitude less than  $10^{-6}$ . As a result, the static moduli show more sensitivity to stress level.

### 2. Porosity effect on the variability of static moduli

Another important feature is that the variations of the static moduli differ a lot for sandstones with different porosities, even at the same stress range. Theoretically, the Voigt-Reuss bound gives the allowable range of the effective elastic moduli (Mavko et al., 2009). However, the isostrain

## Static and dynamic moduli

Voigt bound is unattainable for the nature sedimentary rocks (Mavko et al., 2009). In order to further constrain the potential variability of elastic moduli, the critical porosity ( $\phi_c=40\%$ ) is introduced to modify the Voigt-Reuss bound (Han and Batzle, 2004). According to the feature of the bound models, two endmember components are needed. For dry rocks measured at room-dry conditions, quartz with clay is selected as the component when there is no porosity, while air is treated as the other endmember at the critical porosity. In Equation (5) and (6), M can represent bulk modulus, K, and Young's modulus, E. The bulk modulus ( $K_q$ ) and Young's modulus ( $E_q$ ) for quartz with clay are 39GPa (Han et al., 1986) and 77GPa, respectively. The moduli for air are considered as zero in the calculations.

$$M_V = (1 - \frac{\phi}{\phi_c}) M_q \quad (5)$$

$$M_R = 0 \quad (6)$$

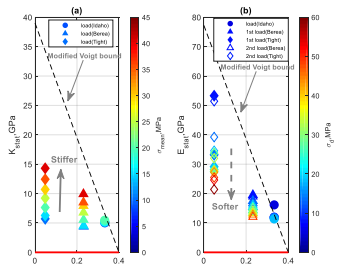


Figure 5. Elastic moduli as a function of porosity at different stress levels, for (a) static bulk moduli and (b) static Young's moduli. The black dashed lines are for modified Voigt bound with critical porosity of 40%. The red solid lines are for modified Reuss bound.

In Figure 5, the static bulk moduli during hydrostatic load and the static Young's moduli during deviatoric load are compared with the theoretical bounds. The modified Voigt bound offers the upper limits of the elastic properties. The distance between these bounds at certain porosity shows the potential variation range of the elastic properties under stress. As a result, with the increase of porosity, the allowable variability of the elastic moduli decreases. All measured data points fall between these two bounds. The amount of modulus variation under stress decreases with the increasing porosity (from Tight to Idaho Gray sandstones). The experimental results are in accordance with the modeling conclusions.

### 3. Stress history effects on the static elastic moduli

We compare the static moduli measured in the loading process with the successive unload. As shown in Figure 6(a), during hydrostatic stage, the unload moduli are always larger than the load ones at any pressure level. With the increase of pressure, the discrepancy between the load and unload bulk moduli presents an increasing trend. As shown in Figure 6(b), in triaxial load-unload cycles, at high stress

level, the unload moduli are higher than the load ones, while the relation is reversed at low stress state. The cross-plot between the load and unload moduli traverses the 1:1 correlation line and shows increasing trends with the elevated stress level.

As mentioned above, the stress increments not only induce elastic and recoverable deformations, they also tend to involve some non-elastic and irrecoverable processes, such as frictional slips, crushing of asperities, and open of microcracks. More importantly, these non-elastic processes are highly dependent on the stress path. Take the frictional slip at a grain contact for instance, this grain contact is constantly subjected to frictional sliding with the elevated stress. At the peak stress, this grain contact again is held together by the static friction. When the load is initially reversed, the grain contact tends to achieve a reversed frictional slip. However, the opposite shear slips will not take place unless the reversed shear forces are built up large enough to overcome the static frictions. Hence, the strain will have a delayed response to the unload, making the unloading curve steeper than the loading one, especially at high stress level. This might be an explanation for the hysteretic behaviors in the stress-strain diagrams and the stress path dependence of static moduli in Figure 6.

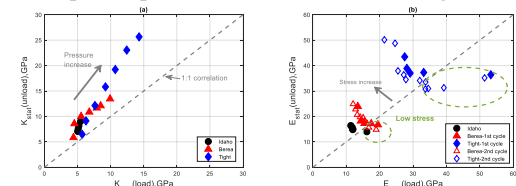


Figure 6. Comparison between load and unload static moduli. The dashed lines are for 1:1 correspondance.

### Concluding remarks

Through the dynamic and static tests on three sandstones with different porosities, we draw the following conclusions:

1. Regardless of being from hydrostatic or triaxial tests, the stress-strain relations show obvious nonlinearity and hysteresis, which could be attributed to the alternation of granular microstructures in the stress load or unload;
2. In contrast to dynamic moduli, the static moduli are more dependent on the stress level, the potential variations of which are constrained by the modified Voigt-Reuss bounds;
3. The statically derived moduli (i.e., bulk and Young's moduli) show strong dependence on the stress history. In general, compared with the loading moduli, the unloading ones, especially at the initial unload, are closer to the dynamic counterparts.

## REFERENCES

- Fjær, E., 2009, Static and dynamic moduli of a weak sandstone: *Geophysics*, **74**, no. 2, WA103–WA112, doi: <https://doi.org/10.1190/1.3052113>.
- Fjær, E., 2019, Relations between static and dynamic moduli of sedimentary rocks: *Geophysical Prospecting*, **67**, 128–139, doi: <https://doi.org/10.1111/1365-2478.12711>.
- Han, D. H., and M. L., Batzle, 2004, Gassmann's equation and fluid-saturation effects on seismic velocities: *Geophysics*, **69**, 398–405, doi: <https://doi.org/10.1190/1.1707059>.
- Han, D. H., A., Nur, and D., Morgan, 1986, Effects of porosity and clay content on wave velocities in sandstones: *Geophysics*, **51**, 2093–2107, doi: <https://doi.org/10.1190/1.1442062>.
- Jaeger, J. C., N. G., Cook, and R., Zimmerman, 2009, Fundamentals of rock mechanics: John Wiley and Sons.
- King, M. S., 1969, Static and dynamic elastic moduli of rocks under pressure: 11th US Symposium on Rock Mechanics. American Rock Mechanics Association.
- Li, H., D. H., Han, J., Gao, H., Yuan, and Y., Wang, 2019, Pressure loading histories and clay fraction effects on the static and dynamic elastic properties of sand-clay synthetic sediments: *Powder Technology*, **345**, 804–814, doi: <https://doi.org/10.1016/j.powtec.2019.01.033>.
- Mavko, G., T., Mukerji, and J., Dvorkin, 2009, The rock physics handbook: Tools for seismic analysis of porous media: Cambridge University Press.
- Simmons, G., and W. F., Brace, 1965, Comparison of static and dynamic measurements of compressibility of rocks: *Journal of Geophysical Research*, **70**, 5649–5656, doi: <https://doi.org/10.1029/JZ070i022p05649>.
- Tutuncu, A. N., A. L., Podio, A. R., Gregory, and M. M., Sharma, 1998, Nonlinear viscoelastic behavior of sedimentary rocks, Part I: Effect of frequency and strain amplitude: *Geophysics*, **63**, 184–194, doi: <https://doi.org/10.1190/1.1444311>.
- Winkler, K., A., Nur, and M., Gladwin, 1979, Friction and seismic attenuation in rocks: *Nature*, **277**, 528–531, doi: <https://doi.org/10.1038/277528a0>.